

Behaviour of joints

Authors: Dr. Van Manh Nguyen & Prof. Dr. habil. Heinz Konietzky, (TU Bergakademie Freiberg, Geotechnical Institute)

1	Introduction.....	2
2	Basic definitions	2
3	Joint Roughness Coefficient measurement techniques.....	5
4	Shear testing devices	9
5	Sample preparation	10
6	Direct shear box testing methods	11
7	Test procedure	12
8	Shear behaviour of intact rock.....	12
9	Behaviour of jointed rock.....	15
9.1	Behaviour of planar joint surfaces	15
9.2	Behaviour of 'saw-tooth' joint surfaces	16
9.3	Behaviour of rough joint surfaces	16
9.4	Dilation behaviour.....	18

1 Introduction

Natural rock masses always contain discontinuities such as joints, fractures, faults, bedding planes and other geological features. The surfaces of such discontinuities can be smooth or rough; in good contact or poor contact; filled or not. Therefore, rock masses are discontinuous and anisotropic materials. The presence of discontinuities in a rock mass has significant influence on its strength, especially shear strength. Also, discontinuities facilitate storage and movement of fluids. Tensile and shear strength of rocks are an important aspect in the design of geotechnical structures such as foundations, slopes, tunnels, shafts, caverns etc.

2 Basic definitions

Joints are discrete brittle fractures in a rock along which there has been little or no movement parallel to the plane of fracture, but slight movement normal to it (see fig. 1)[Allaby 2008].

Orientation of a discontinuity is described by its dip and dip direction or strike. Dip of a plane is measured by the degree of inclination (actual angle between the discontinuity surface and the horizontal plane). Dip angle is within the range of 0° to 90° . Dip direction is the facing direction and is measured clockwise from true North. Dip direction is generally expressed by a direction angle between 0° to 360° . Strike is the alignment and is always perpendicular to the dip direction. Strike is generally expressed by a direction angle between 0° to 180° .



Fig. 1. Columnar joints [Geology Field Camp 2017]

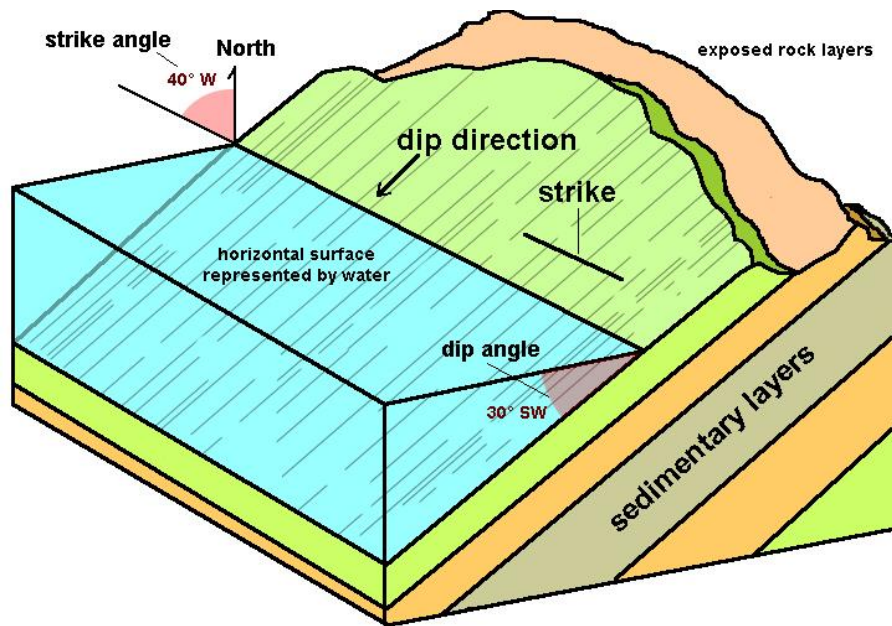


Fig. 2. Describing orientation of geologic features [Geology Café 2013]

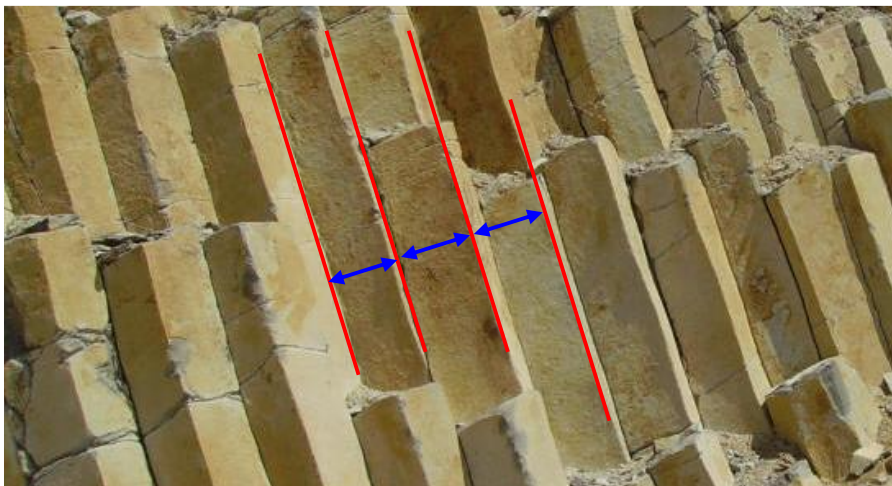


Fig. 3. Joints spacing [modified after Geology Field Camp 2013]

Spacing is the perpendicular distance between adjacent discontinuities, and is usually expressed as the mean spacing of a particular set of joints. The spacing of discontinuity is largely controlled by the size of individual blocks of intact rock and mode of failure.

Roughness is a measure of the inherent surface unevenness and waviness of the discontinuity relative to its mean plane. The roughness is characterized by large scale waviness and small scale unevenness of a discontinuity. It is a major factor governing the shear displacement and shear strength. A commonly used parameter is based on the roughness classification proposed by Barton and called JRC (Joint Roughness Coefficient). JRC number is 0 for smooth flat surfaces and 20 for very rough surfaces. Joint roughness is affected by geometrical scale.



Fig. 4. Classical profilometer for measuring the roughness profile of rock samples [ControlsGroup 2013]

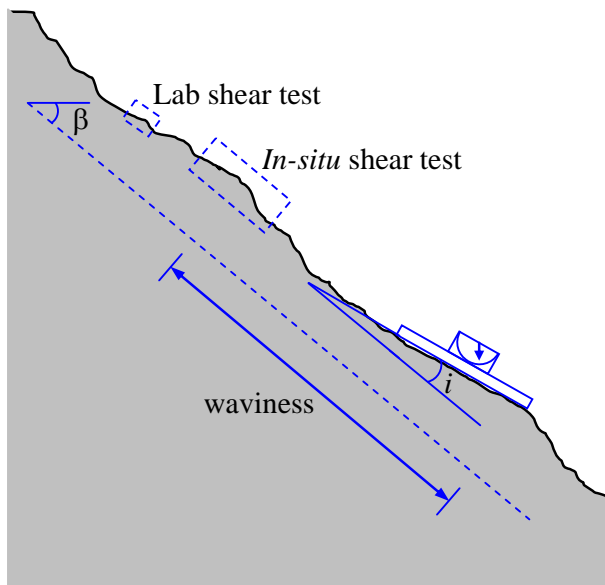


Fig. 5. Definition of joint roughness at different scale

Open and filled joints: In natural joints, it is very seldom that the two surfaces match completely. Usually a gap or opening exist between the two surfaces (open or partly open joint). The interface can be filled with air, water or filling material (filled joint) such as calcite, clay, quartz or pyrite, etc.

Aperture is the perpendicular distance separating the adjacent rock walls of an open discontinuity. Therefore, aperture has to be distinguished from the width of a filled discontinuity.

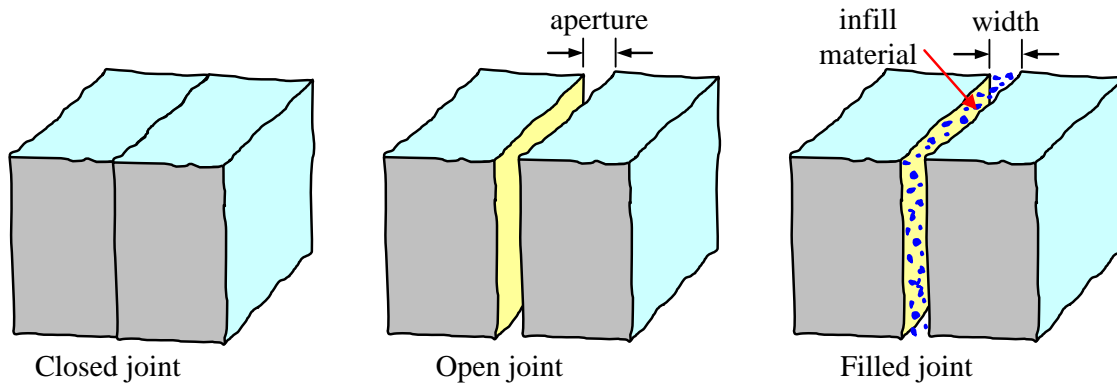


Fig. 6. Joint aperture and joint filling

3 Joint Roughness Coefficient measurement techniques

The shear strength of rock joints is strongly dependent on the surface roughness. Therefore, it is important to estimate the roughness of discontinuity surface accurately. The **Joint Roughness Coefficient (JRC)** is a commonly used measure of joint roughness in rock engineering practice. Roughness can be subdivided into small scale surface irregularities and large scale undulations of the discontinuity surface.

Several methods have been developed and used to measure rock joint surface roughness in-situ and in the laboratory. These methods can be divided into two categories: requiring contact with the rock joint surface termed “Contact methods” and not requiring contact with the rock joint surface termed “Non-Contact methods” [Maerz et al. 1990].

Contact methods: Several instruments and methods, respectively, have been developed to measure the surface roughness of rock discontinuities:

- the linear profiling method
- the compass and disc-clinometer method
- the profile combs method
- the straight edge and rulers method
- the shadow profilometry method
- the tangent plane and connected pin sampling method

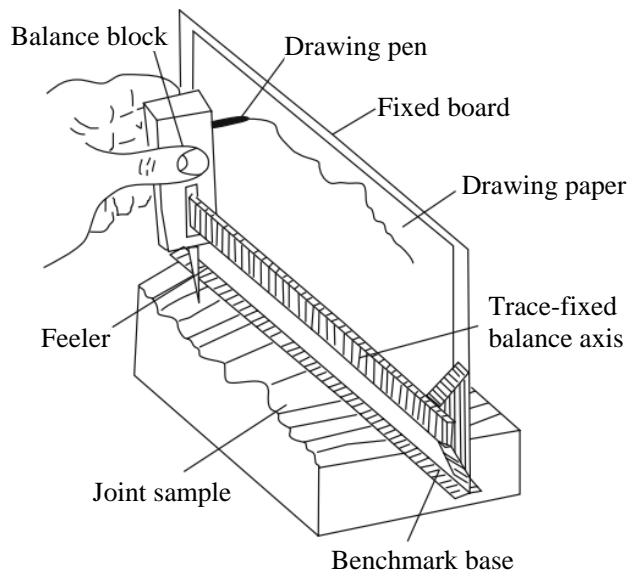


Fig. 7. Simple profilograph for measurement of joint roughness [Shigui et al. 2009]

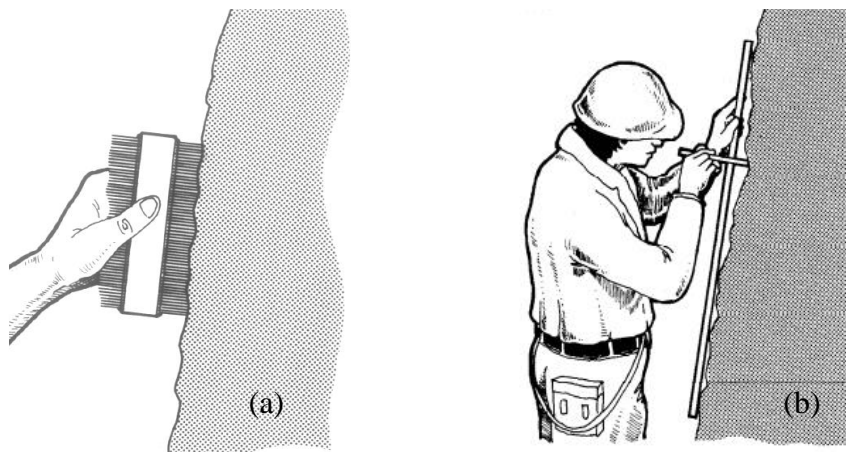


Fig. 8. Example of contact methods for measurement of joint surface roughness [Milne et al. 1991]

(a): use of a profile comb to measure discontinuity roughness profiles.

(b): use of straight edge method to measure the waviness of rock discontinuity

The contact methods have the advantage to be cheap, accurate, easy to handle and suitable to measure large scale roughness in the field [Maerz et al. 1990, Fecker & Rengers 1971, Rasouli & Harrison 2004, Schmittbuhl et al. 1993] or small scale roughness in the laboratory [Weissbach 1978, Kulatilake et al. 1995]. However, contact methods also have some disadvantages: they are time-consuming when used to measure large areas and they do not allow for data recording at dangerous and inaccessible locations [Feng et al. 2003]. These drawbacks can be overcome by using non-contact methods to measure discontinuity surface topography.

Non-Contact methods: There are several non-contact measurement instruments and methods, respectively, available to obtain 2D and 3D rock joint surface topography, for example:

- the photogrammetry method
- the image processing method
- the advanced topometric sensor method
- the laser scanning

Application of photogrammetry for measurement of rock joint surface roughness was first proposed by Wickens and Barton (1971) and ISRM (1978). In recent years, several researchers have developed close-range photogrammetry to measure discontinuity surface roughness in the laboratory [Jessell et al. 1995, Lee & Ahn 2004, Nilsson et al. 2012] and in-situ [Haneberg 2008, Baker et al. 2008, Poropat 2009]. The advanced topometric sensor method has been developed and manufactured by GOM mbH and is intensively used to digitize rock discontinuity surfaces [Grasselli & Descoeurdes 2001, Hong et al. 2008, Nasserri et al. 2009, Chae et al. 2004]. 3D-scanning technique is a sophisticated active remote sensing technique that has been used recently to measure more accurate discontinuity surface roughness in the field [Poropat 2009, Fardin et al. 2004, Hong et al. 2006, Tatone & Grasselli 2009]. These methods greatly improved the speed and accuracy of roughness measurements. However, many of these methods can only be used in the laboratory for measuring small specimens [Poropat 2009, Tonon & Kottenstette 2006]. Fig. 10 illustrates an example of using 3D-scanner device for capturing rock surface topology.

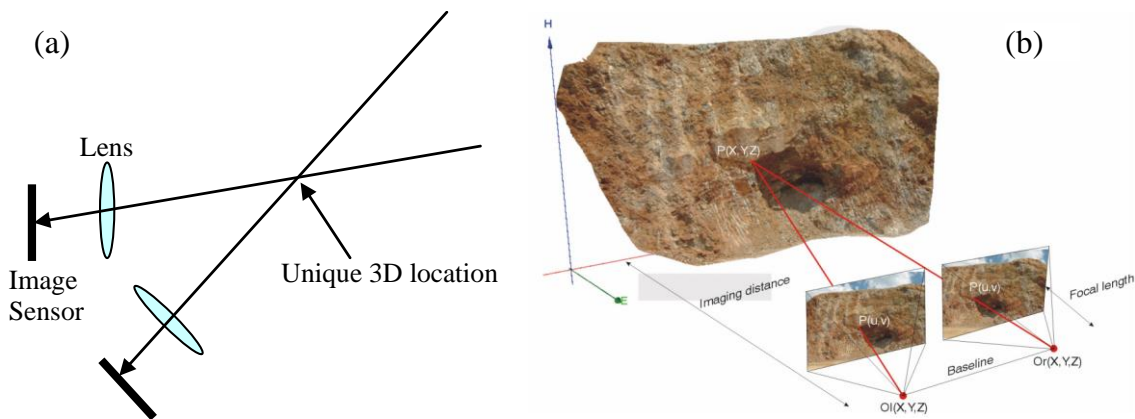


Fig. 9. Principle of photogrammetry [Birch 2006, Gaich et al. 2006]

- simplified scheme showing the process of finding the unique 3D location of the intersection of rays projected from two 2D images
- Concept illustrated via two 2D photographs of a rock mass.

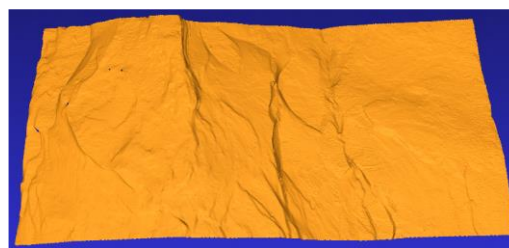


Fig. 10. Example of using 3D-scanner device for capturing rock surface features [Nguyen 2013]

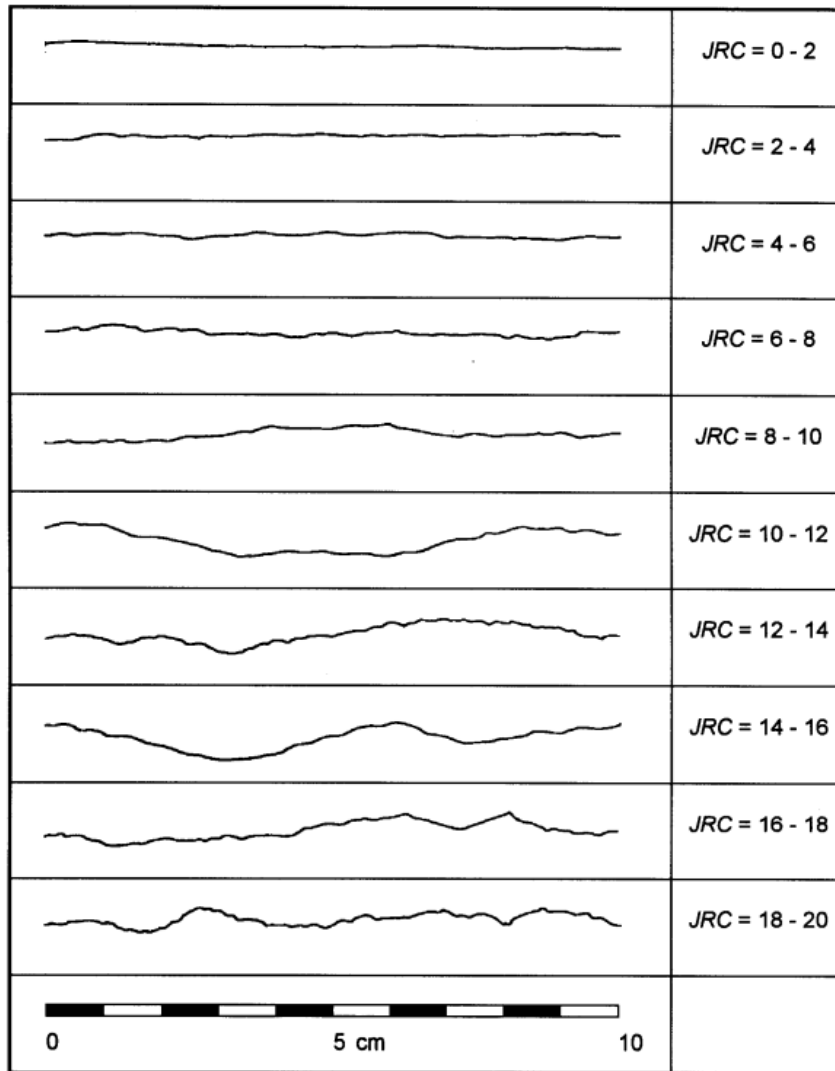


Fig. 11. JRC profiles proposed by Barton (1976)

The JRC value of a rock joint can be estimated visibly by comparing it with the 10 standard JRC profiles (Fig. 11), which were proposed by Barton (1976). However, it may be difficult to determine the proper JRC number in practice, because of the scale effect. At present, many researchers [Tatone & Grasselli 2009, Tse & Cruden 1979, Yang et al. 2001, Belem et al. 2000] have proposed methods to calculate the JRC value from the profile geometry of scanned surface.

4 Shear testing devices

The most commonly used method for testing the shear behaviour of rock joints is the direct shear test. This type of test is usually carried out in the laboratory, but it may also be performed in the field. In recent years, several commercial producers have developed shear box devices for rock mechanical testing (e.g. MTS-816, GCTS-RDS-500, TerraTek-DS-4250, LO-5010, HR72.340). Beside that, several researchers [Geertsma 2002, Gehle 2002, Seidel & Haberfield 2002, Jiang et al. 2004, Kim et al. 2006, Gomez et al. 2008, Barla et al. 2010, Konietzky et al. 2012a, Konietzky et al. 2012b, Nguyen 2013] have designed and constructed their own shear box devices to perform direct shear tests. The technical data show maximum normal forces of 1500 kN; maximum shear forces of 800 kN and maximum shear box dimensions of 200 x 400 mm.

In addition, the triaxial cell is sometimes used to investigate the shear strength of discontinuities in rock. The triaxial cell is well suited for testing discontinuities in the presence of water and core specimens containing discontinuities inclined at 25-40° to the specimen axis. The specimen is set-up in the triaxial cell as shown in Fig. 12. Tests can be performed under drained or undrained conditions, preferably with a known level of joint water pressure being imposed and maintained throughout the test. In order to allow slip on the joint surface, one spherical seat (Fig 12b) or two spherical seats (fig 12c) are used in the system or a pair of hardened steel discs are inserted between the platens and either end of the sample.

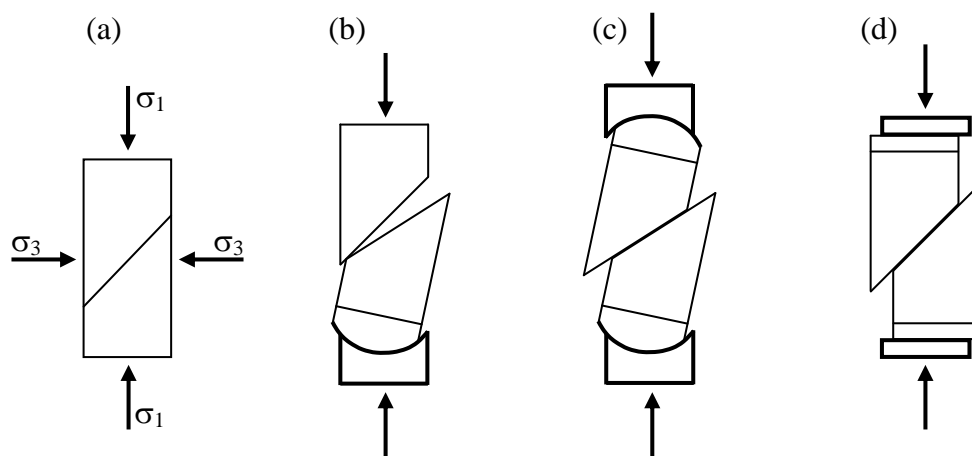


Fig. 12. Shear testing in a triaxial cell [Jaeger & Rosengren 1969]

5 Sample preparation

Direct shear tests can be performed on intact or jointed rock samples. The sample should be prepared (cut) in such a way, that it fits into the shear box. The sample has to be fixed (grouted) inside the steel shear box. The strength of the fixing material should be larger than that of intact material of the sample. The sample is then left for at least 48 hours to let the grout drying. Fig. 13 shows the intact rock specimen preparation for direct shear testing.

In case of existing joint, the discontinuity surface is aligned parallel to the shear direction. The two halves of the sample are also fixed inside the upper and lower shear box. The cross-sectional area of the specimen and the roughness should be measured before grouting carefully.



a) Intact sample



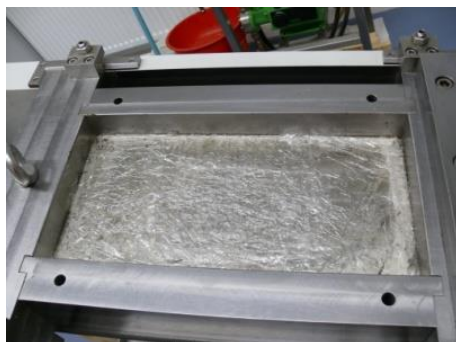
b) Shear box



c) Sample in the shear box



d) Grouted sample



e) Grout drying



f) LVDTs for displacement measurement

Fig. 13. Intact rock specimen preparation for shear testing (Nguyen 2013)

6 Direct shear box testing methods

Direct shear box tests are carried out in the laboratory to determine shear strength of intact rock and jointed rock under static or dynamic boundary conditions. There are two main methods usually used in the laboratory to investigate the shear behaviour of rock joints under quasi-static conditions. They are called **Constant Normal Load (CNL)** and **Constant Normal Stiffness (CNS)** tests.

CNL means that the normal load is maintained constant during the shearing process. Shear testing under CNL boundary conditions is only suitable for cases such as non-reinforced rock slopes, where the surrounding rock mass freely allows the joint to shear without restricting the dilation (Fig. 14a).

CNS means that the normal stiffness is maintained constant during the shearing process. Shear testing under CNS boundary conditions is usually suitable to investigate the behaviour in deep underground openings or rock bolt reinforced slopes, where the surrounding rock mass is unable to deform sufficiently and the normal stress acting on the shear plane is not kept constant during the shearing process. In this case, the dilation is controlled by the normal stiffness of the surrounding rock mass (fig. 14b).

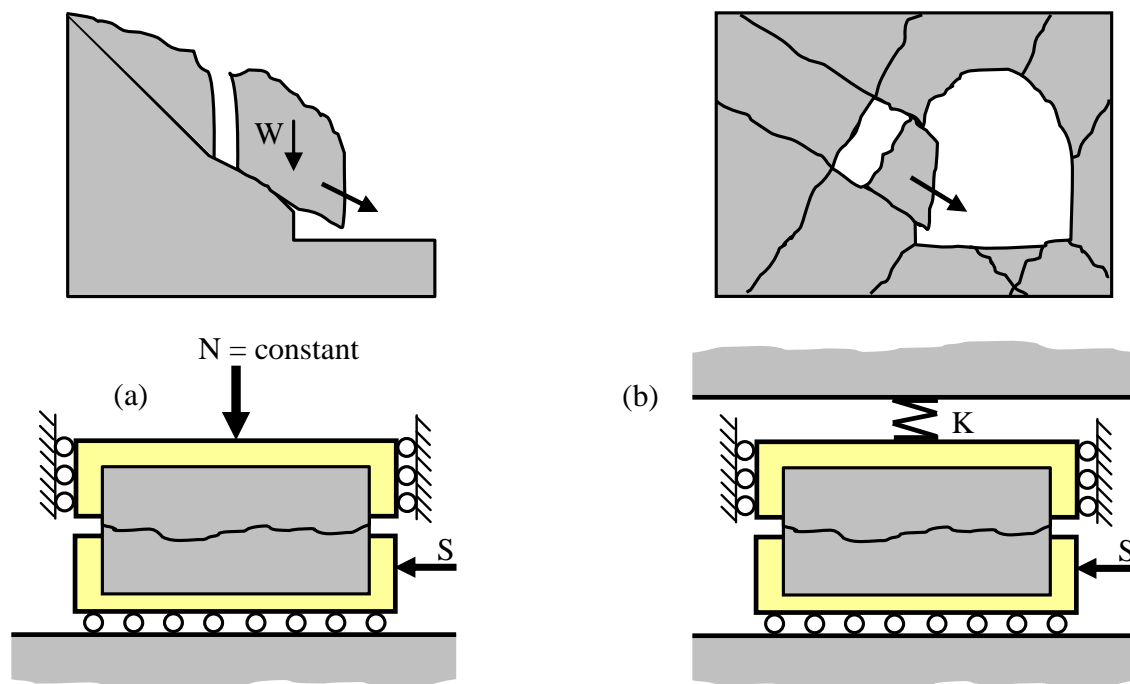


Fig. 14. Simulation of the in-situ boundary conditions in the direct shear test

7 Test procedure

The test procedure described within this chapter corresponds to the procedure and the device used by Konietzky et al. (2012a, 2012b) and Nguyen (2013).

Measuring devices: horizontal and vertical displacements are measured by LVDT's (Linear Variable Differential Transformer). Vertical displacements are measured at the four corners at the upper shear frame. Horizontal displacement is measured by a LVDT fixed to the lower shear box part. The normal load is measured by a load-cell integrated into the vertical load piston. The shear load is measured by another load-cell connected to the horizontal load piston. Therefore, external measurements direct at the sample and machine internal measurements are available.

Data acquisition Equipment: Two computers are used to control the direct shear test, to collect and visualize data and graphs during the experiment.

Application of the normal force (CNL-test): the normal load is continuously increased until the prescribed constant value of normal load is reached. Normal displacements are recorded during this process. The constant normal load is held constant during shear testing.

Application of the shear force (CNL-test): a selected shear rate is applied. After reaching the peak shear strength, shear loading acts until residual strength is reached. Normal and shear displacements are measured with the four vertical LVDT's and the horizontal LVDT in addition to the vertical and horizontal force measurements.

8 Shear behaviour of intact rock

Shear strength is the resistance to deformation by continuous shear displacement upon the action of shear stress. Shear strength of rock is the sum of surface frictional resistance to sliding, interlocking effect between the individual rock grains and natural apparent cohesion.

The peak shear strength is the highest stress sustainable just prior to complete failure of sample under shear load; after this, stress cannot be maintained and major strains usually occur by displacement along failure surfaces. The peak shear strength of a rock joint undergoing shear displacement is dependent on the normal load applied across the interface, surface characteristics such as roughness and joint wall strength, and the boundary conditions.

The residual shear strength is the ultimate strength along a surface in rock after shearing has occurred. The residual shear strength typically depends on the applied normal stress.

Suppose that three samples of intact rock are used for shear testing. The set-up for intact rock sample testing under CNL condition is illustrated in Fig. 15. Shear box tests are performed until peak shear strength is reached. The vertical load is maintained constantly during shear process.

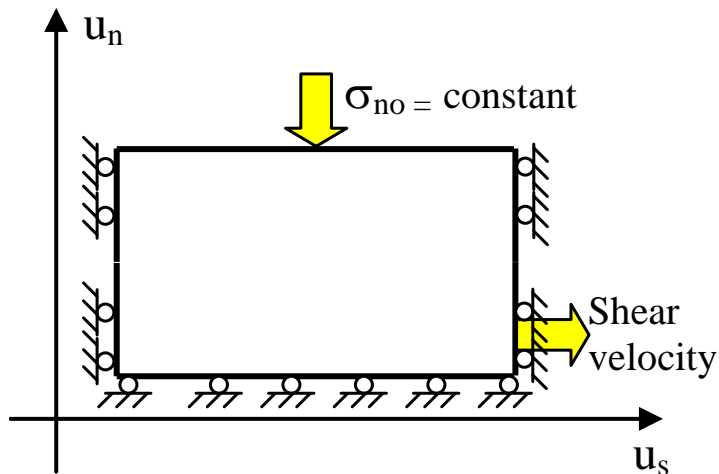


Fig. 15. CNL test set-up for intact sample

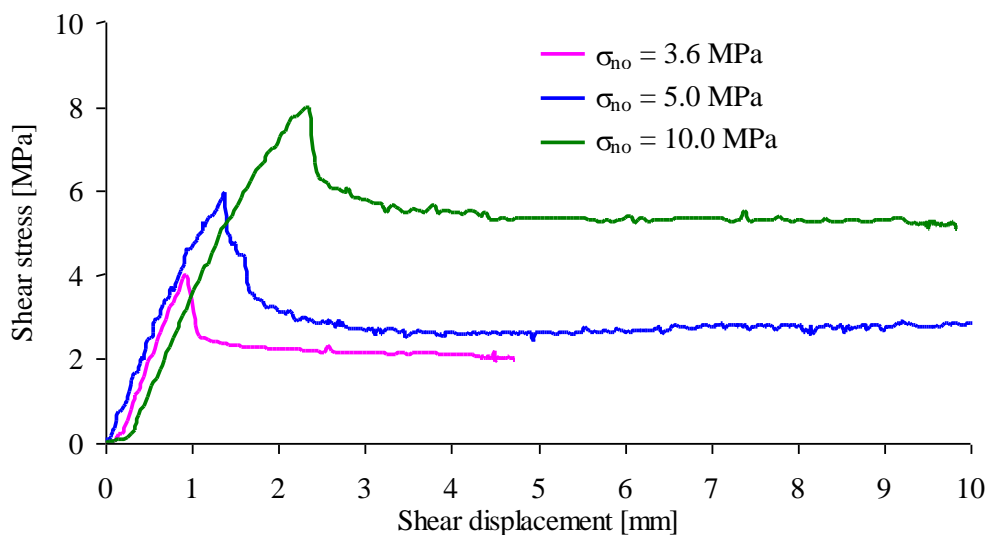


Fig. 16. Shear stress versus shear displacement under different normal stress for intact rock specimens

The shear behaviour of intact rock obtained throughout the direct shear tests under various normal stresses are shown in Fig. 16. The peak and residual shear stresses of rock joints can be determined from these curves. Fig. 16 shows that shear stress of intact rock increases linearly (elastic behaviour) with increasing shear displacement until peak shear strength is reached. After that the shear stress decreases until the residual shear strength (plastic behavior) is reached. Peak and residual shear strength of intact rock increase also with increasing normal load. The peak shear strength is obtained at higher shear displacement when normal stress increases as shown in Fig. 16.

The peak and residual shear stress values for different normal stresses are shown in Fig. 17. The relationship between the peak shear stress and the initial normal stress can be represented by the Mohr-Coulomb failure envelop:

$$\tau_{\text{int-p}} = \sigma_{no} \tan(\phi_{\text{int-p}}) + c_{\text{int}}$$

where τ_{int-p} is the peak shear stress of the intact rock
 σ_{no} is the initial normal stress
 ϕ_{int-p} is the peak internal friction angle of the intact rock
 c_{int} is the cohesion of the intact rock.

The cohesion in the case of the residual state has dropped to zero and the relationship between the residual shear stress and the initial normal stress can be represented by:

$$\tau_{int-r} = \sigma_{no} \tan(\phi_{int-r})$$

where τ_{int-r} is the residual shear stress of the intact rock
 ϕ_{int-r} is the peak internal friction angle of the intact rock.

The other mechanical parameters of intact rock such as cohesion and friction angle can also be determined by the Mohr-Coulomb failure envelopes.

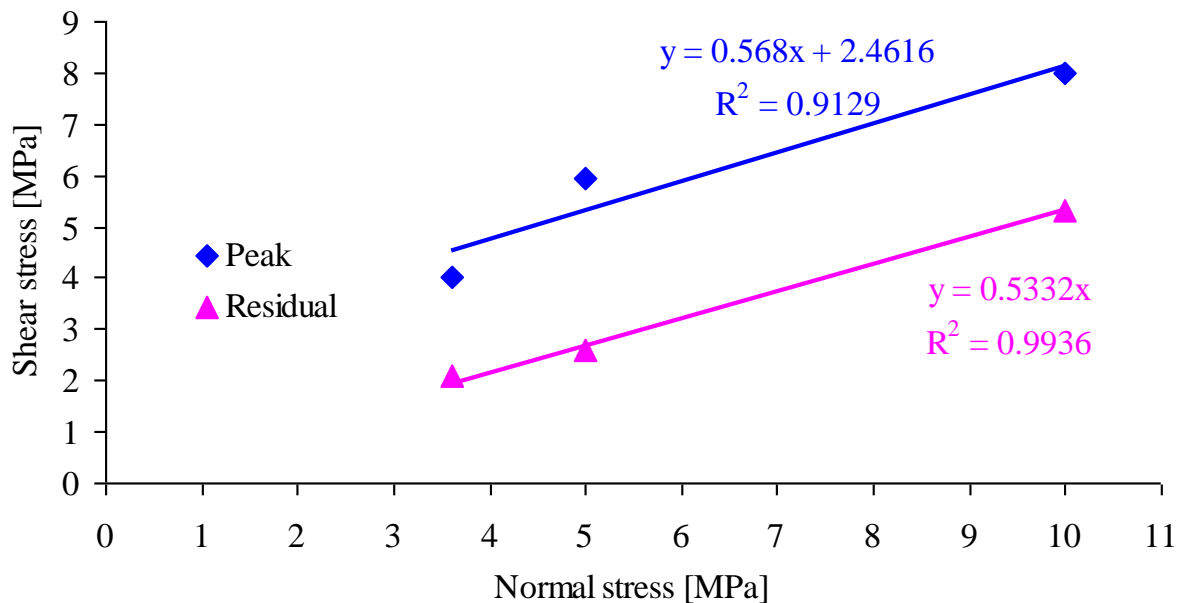


Fig. 17. Mohr-Coulomb failure envelope for peak and residual state for initial intact rock samples

9 Behaviour of jointed rock

9.1 Behaviour of planar joint surfaces

The typical shear behaviour of planar joint surfaces is illustrated in Fig. 18. The shear stress increases rapidly until the peak shear stress is reached. Then the shear stress decreases to some residual value that remain constant even for large shear displacement. The relations between peak or residual shear stresses and different normal stresses are plotted in Fig. 18. The line for peak shear stress has a slope of ϕ_p and an intercept of c on the shear stress axis. The line for residual stress has a slope of ϕ_r .

The relationship between the peak shear stress and the initial normal stress for rock joints can be represented by the Mohr-Coulomb failure criterion:

$$\tau_p = \sigma_{no} \tan(\phi_p) + c$$

where τ_p is the peak shear stress of the jointed rock
 ϕ_p is the peak internal friction angle of the jointed rock
 C is the cohesion of the jointed rock.

The cohesion at the residual shear stress level has dropped to zero, therefore, the relationship between residual shear stress and normal stress can be represented by following equation:

$$\tau_r = \sigma_{no} \tan(\phi_r)$$

where τ_r is the residual shear stress of the jointed rock
 ϕ_r is the residual internal friction angle of the jointed rock.

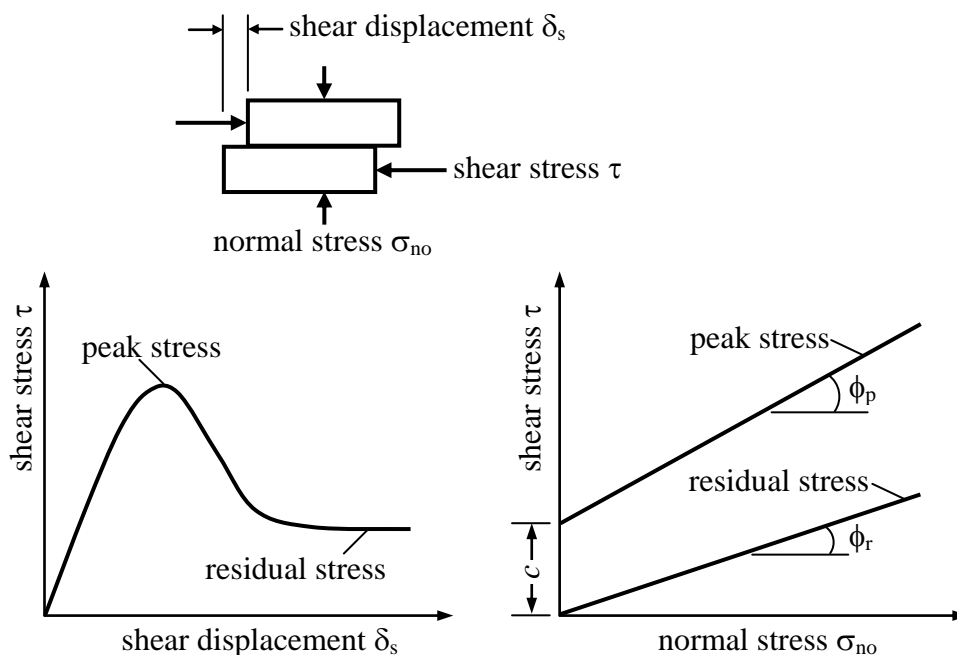


Fig. 18. Shear behaviour of planar joint surfaces

9.2 Behaviour of 'saw-tooth' joint surfaces

Patton (1966) carried out shear tests on 'saw-tooth' specimens under low normal stress as illustrated in Fig. 19. Shear displacement in these specimens occurs as a result of the surfaces moving up the inclined faces, causing dilation (increase in volume).

The shear strength of Patton's 'saw-tooth' specimens can be represented by

$$\tau_p = \sigma_{no} \tan(\phi_b + i)$$

where i is the angle of the 'saw-tooth' face
 ϕ_b is the basic friction angle ($\phi_b \approx \phi_r$).

9.3 Behaviour of rough joint surfaces

The discontinuity surfaces in hard rock are never smooth but they are always rough. The surface roughness of natural rock joints is an extremely important parameter, which has influence on several aspects of the shear behaviour of joints, especially in the case of unfilled joints. Generally, the shear strength of the joint surface increases with increasing surface roughness. Barton (1976) has proposed a joint roughness coefficient (JRC) to take care of the strength of discontinuities in rock mass (Q - system) as shown in Fig. 11.

Shear behaviour of rough rock joints is illustrated in Fig. 20. Depending on the types of rocks the difference between peak and residual shear stresses may be significant or not. The red curve in Fig. 20 indicates that the residual shear stress is significantly lower than the peak shear stress (brittle behavior). However, the blue curve shows that the residual shear stress is only slightly lower than the peak shear stresses. This is typical behaviour of ductile rock joints [Grasselli 2001].

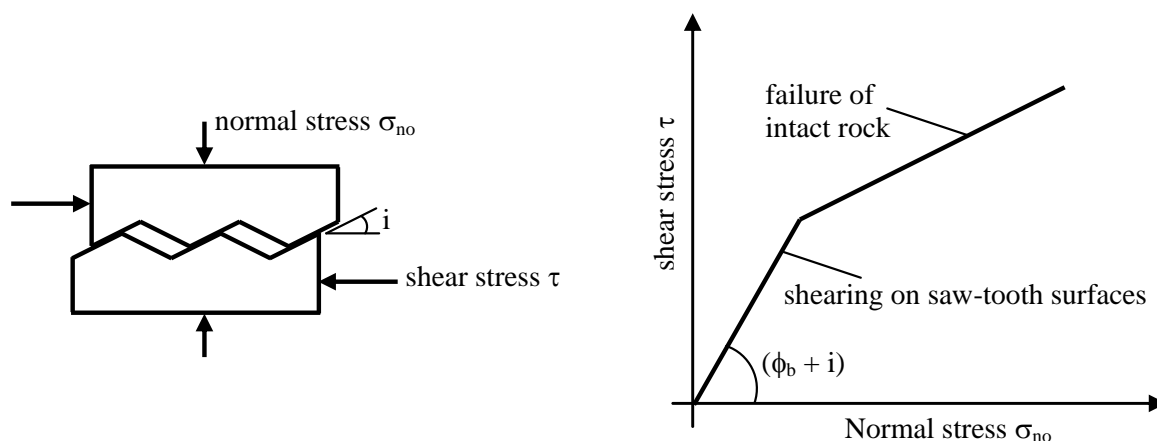


Fig. 19. Patton's experiment on the shear strength of 'saw-tooth' specimens

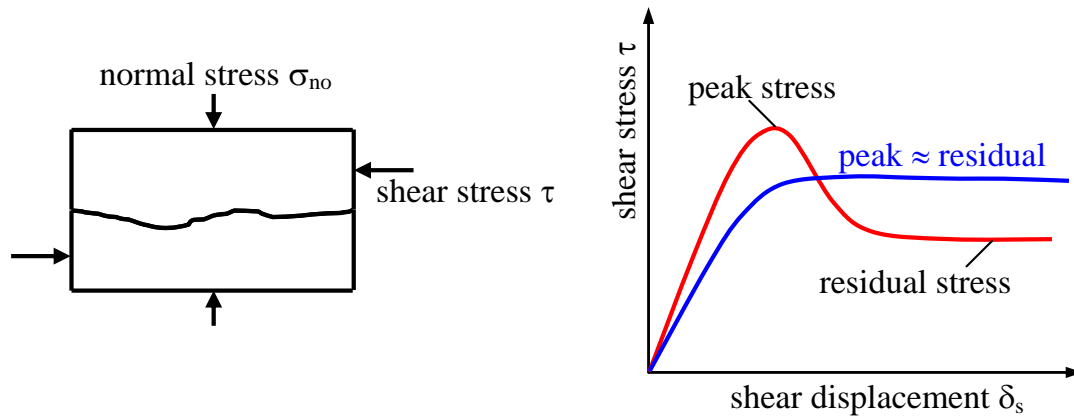


Fig. 20. Shear behaviour of rough rock joints

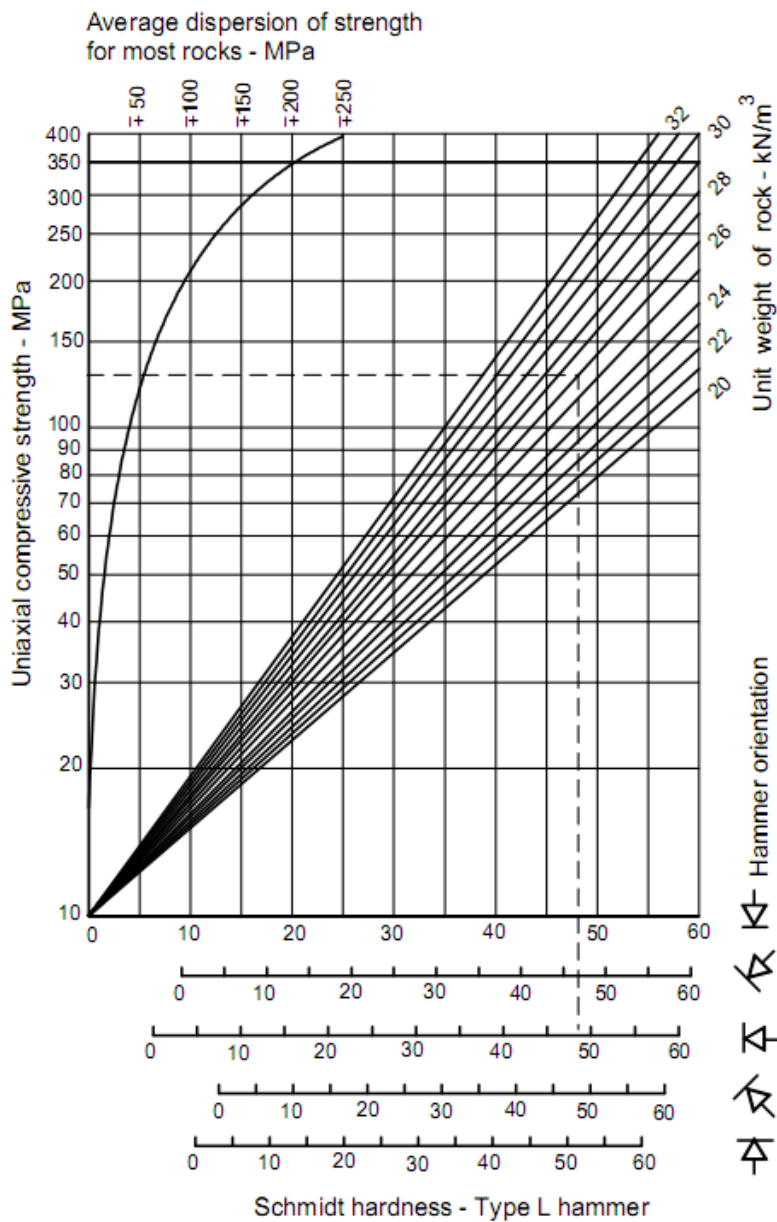


Fig. 21. Estimation of joint wall compressive strength (JCS) from Schmidt hardness (Deere & Miller 1966)

The relationship between shear stress, initial normal stress and JRC can be represented by Barton's equation:

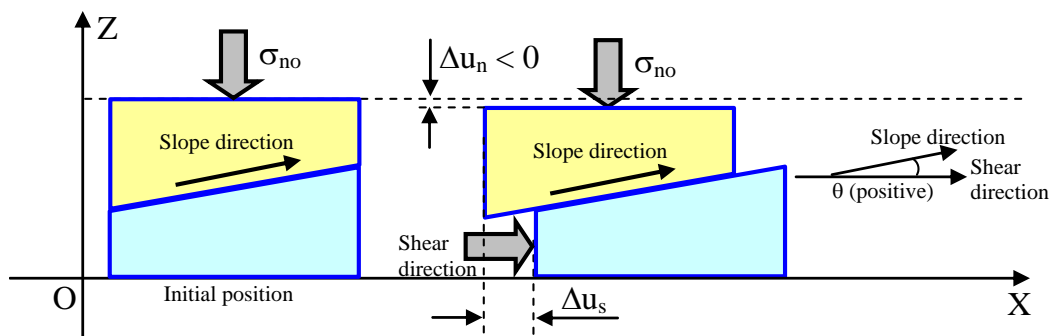
$$\tau = \sigma_{no} \tan \left(\phi_b + JRC \log_{10} \left(\frac{JCS}{\sigma_{no}} \right) \right)$$

where JRC is the joint roughness coefficient
 JCS is the joint wall compressive strength.

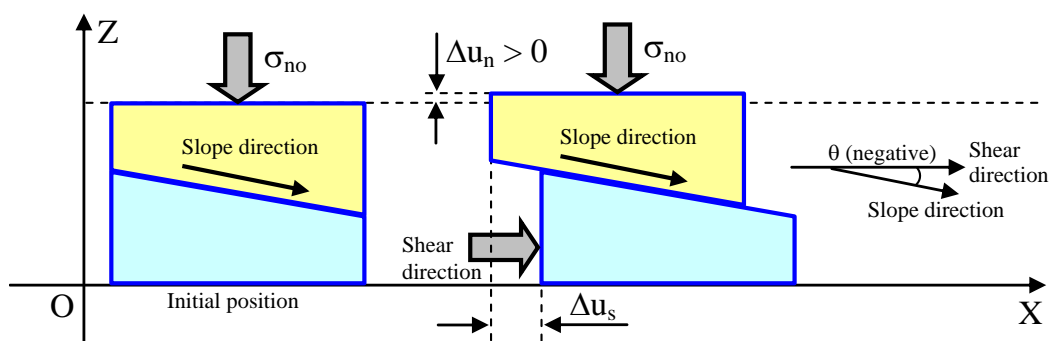
The joint wall compressive strength is estimated by using the Schmidt rebound hammer, which was proposed by Deere and Miller (1966) as illustrated in Fig. 21. The technique considers the unit weight of rock, hammer orientation and Schmidt hardness.

Quit similar to the case of the intact rock, the Mohr-Coulomb failure envelope can also be drawn using the results of peak shear stress under different normal stresses. The friction angle and cohesion of rough rock joint can be obtained as the inclination of this straight line and the intercept on the vertical axis, respectively.

9.4 Dilation behaviour



a) Angle (θ) is positive (negative dilation, $\Delta u_n < 0$)



b) Angle (θ) is negative (positive dilation, $\Delta u_n > 0$)

Fig. 22. The relationship between shear direction and slope direction of interface

In general the dilation angle (ψ) is defined as the ratio of incremental normal displacement to incremental shear displacement as follows:

$$\tan \psi = \frac{\Delta u_n}{\Delta u_s}$$

where Δu_n is the increment of normal displacement,
 Δu_s is the increment of shear displacement.

Generally, the dilation potential of rock joints decreases with the increase of the applied normal stress. However, depending on the relationship between shear direction and slope direction of interface as shown in Fig. 22, the dilation angle can be positive or negative. The experimental results indicate the negative and positive dilation behaviour are shown in Fig. 23 and Fig. 24, respectively.

The dilation behaviour depends on the level of applied normal stress. Increasing applied normal stress leads to a decrease of the dilation angle for both negative and positive dilation as shown in Fig. 23 and Fig. 24, respectively. There are techniques available to transfer the dilational behaviour into a plane parallel to the shear direction (Nguyen 2013). This allows to use the dilation angle in a generalized manner. It should be noted, that dilation and therefore also dilation angle is not constant during the shearing process, but gradually decreases until it approaches nearly zero for large shear displacements.

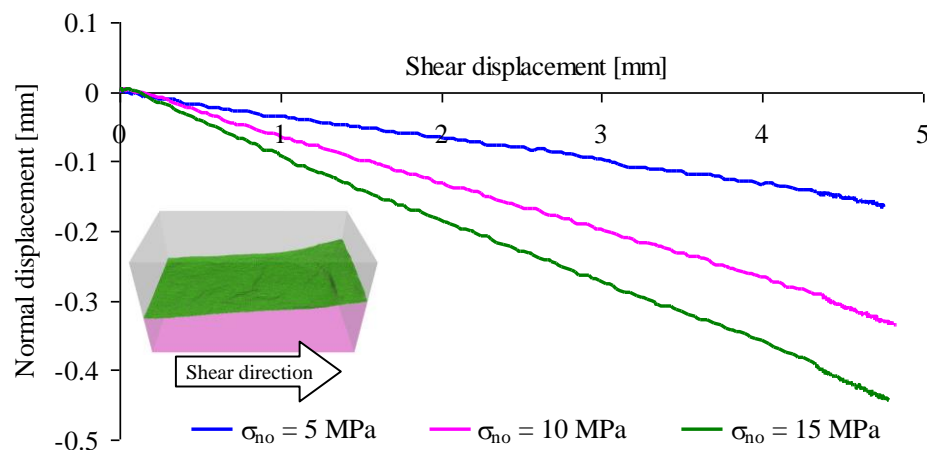


Fig. 23. Negative dilation behaviour of rock joints

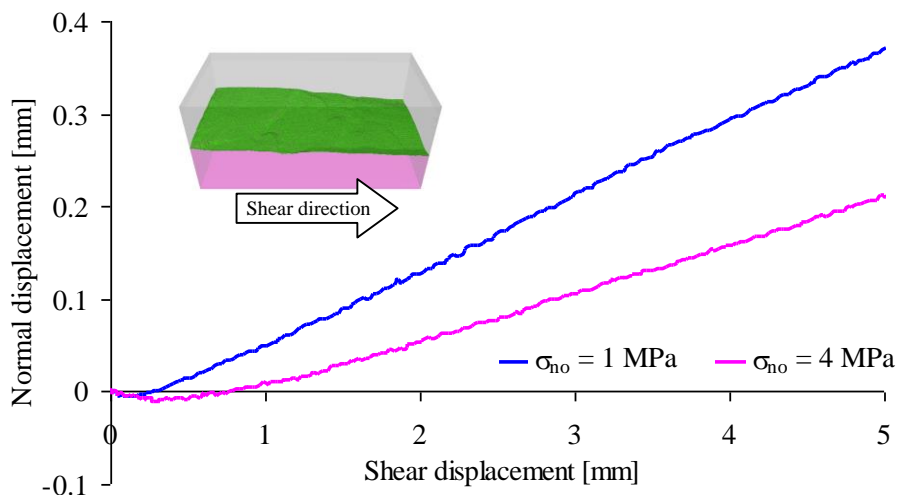


Fig. 24. Positive dilation behaviour of rock joints

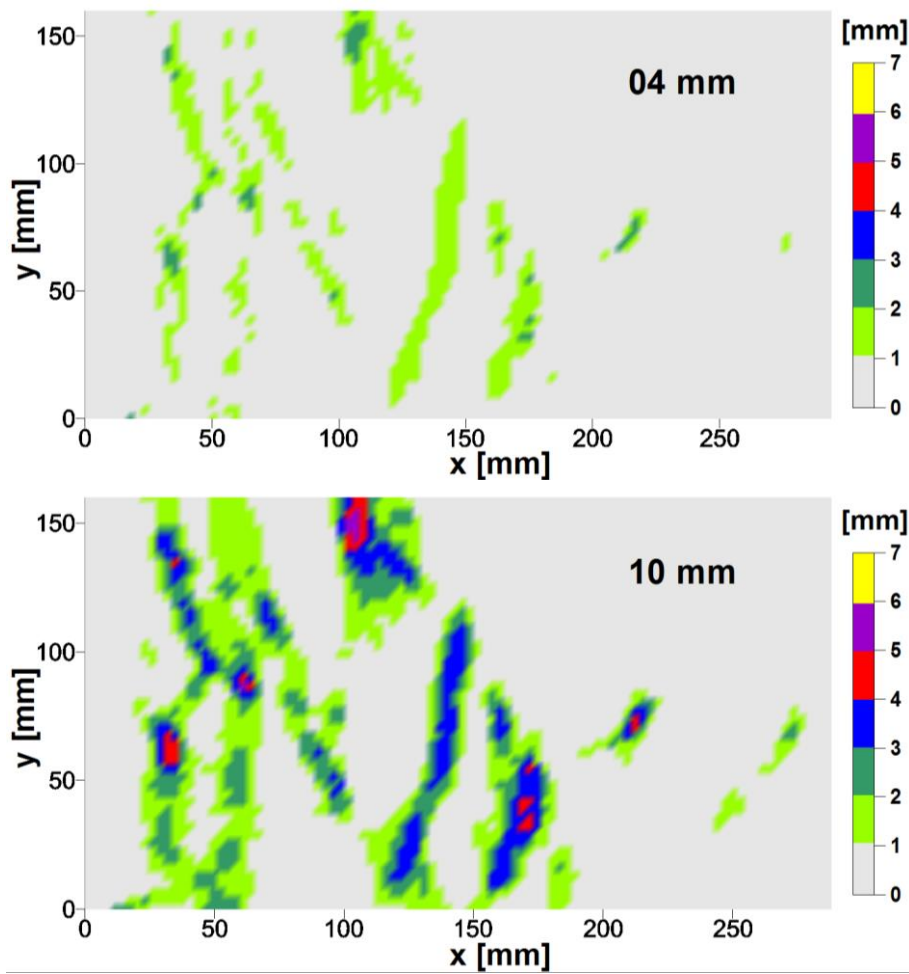


Fig. 25: Measured aperture size distribution for joint at 5 MPa normal stress and 4 and 10 mm shear displacement, respectively (Nguyen 2013).

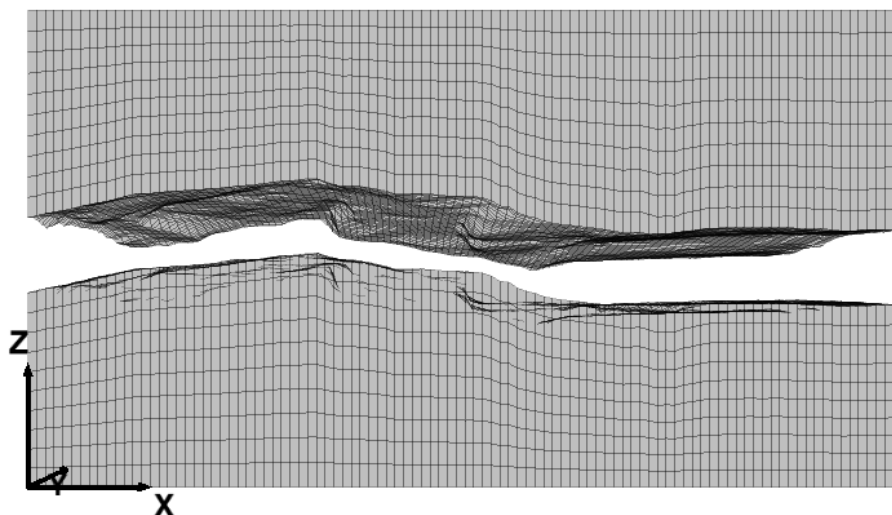


Fig. 26: Numerical model with explicit consideration of surface roughness to simulate shear box test for sample CNL01 (Nguyen 2013)

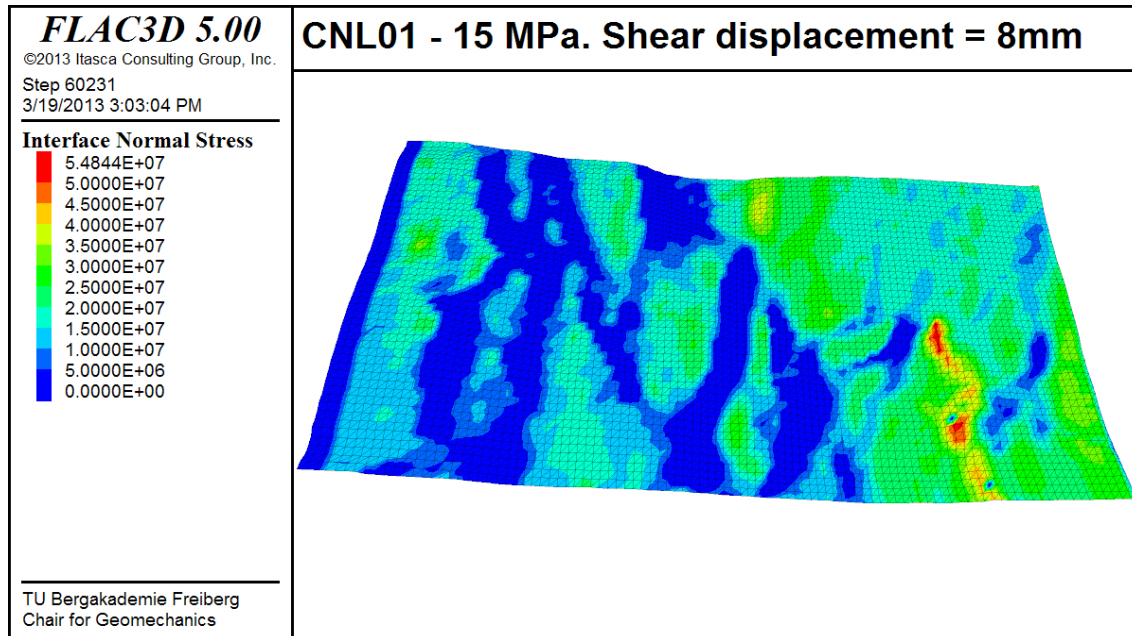


Fig. 27: Normal stress distribution [Pa] at the shear plane at 8 mm shear displacement and 15 MPa normal stress obtained by numerical simulation for sample CNL01 (Nguyen 2013)

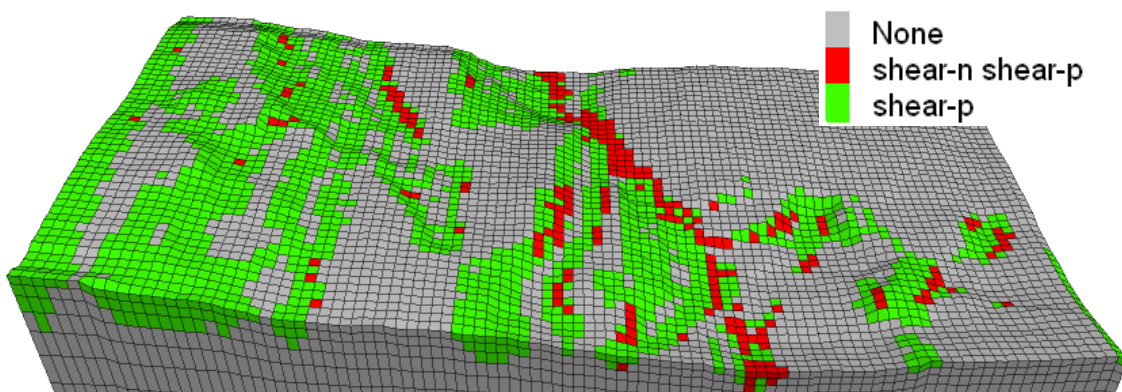


Fig. 28: Plasticity state at shear displacement of 15 mm and normal stress of 15 MPa for sample CNL01 (Nguyen 2013)

The roughness of joints leads to the circumstance, that with ongoing shear displacement a permanent change of local fracture aperture and local stresses occur. Local stresses can reach a multiple of the applied normal stresses and can lead to significant breakage of asperities and therefore ongoing change in joint topology. Exemplary, fig. 25 shows the measured aperture size distribution for a joint during the shearing process.

As figures 26 to 28 indicate exemplary, due to the joint roughness the normal stress distribution is very inhomogeneous and can reach very high local values, which can lead to damage of asperities.

References

- Allaby, M. (2008): *A dictionary of Earth sciences*, third edition, Oxford University press.
- Baker, B.R.; Gessner, K.; Holden, E.J. & Squelch, A.P. (2008): Automatic detection of anisotropic features on rock surfaces. *Geosphere*, 4(2): 418-428.
- Barla, G.; Barla, M. & Martinotti, M.E. (2010): Development of a new direct shear testing apparatus. *Rock mechanics and Rock engineering*, 43(1): 117-122.
- Barton, N.R. (1976): The shear strength of rock and rock joints. *Int J Rock Mech Min Sci Geomech Abstr*, 13(9): 255-279
- Belem, T.; Homand-Etienne, F. & Souley, M. (2000): Quantitative parameters for rock joint surface roughness. *Rock mechanics and Rock engineering*, 33(4): 217-42.
- Birch, J. S. (2006): Using 3DM analyst mine mapping suite for rock face characterization, In: *Laser and photogrammetric methods for rock face characterization*, Tonon F., and Kottenstette, J.T., (Eds), The 41st U.S. Rock Mechanics Symposium, Colorado School of Mines, Golden, Colorado, p. 13-32.
- Chae, B. G.; Ichikawa, Y.; Jeong, G.C.; Seo, Y.S. & Kim, B.C. (2004): Roughness measurement of rock discontinuities using a confocal laser scanning microscope and the Fourier spectral analysis. *Engineering Geology*, 72(3-4): 181-199.
- ControlsGroup (2013): Rock Mechanics - Profilometers (Barton Comb). <http://www.controls-group.com/eng/rock-mechanics-testing-equipment/profilometers-barton-comb.php>, last accessed 06.12.2018.
- Deere, D. & Miller, R. (1966): Engineering classification and index properties for intact rock. *Tech. Report No AFWL - TR-65-116*, Air Force Weapons Lab., Kirtland Air Base, New Mexico.
- Fardin, N.; Feng, Q. & Stephansson, O. (2004): Application of a new in-situ 3D laser scanner to study the scale effect on the rock joint surface roughness. *Int. J. Rock Mech. Min. Sci.*, 41(2): 329-335.
- Fecker, E. & Rengers, N (1971): Measurement of large-scale roughness of rock planes by means of profilograph and geological compass. *Rock Fracture, Proc. of Int. Symp. Rock Mech*, Nancy. p. 1-18.
- Feng, Q; Fardin, N; Jing, L & Stephansson, O (2003): A new method for in-situ non-contact roughness measurement of large rock fracture surfaces. *Rock mechanics and Rock engineering*, 36(1): p. 3-25.
- Gaich, A.; Pötsch, M. & Schubert, W (2006): Basics and application of 3D imaging psystems with conventional and high-resolutions cameras, in *Laser and photogrammetric methods for rock face characterization. The 41st U.S. Rock mechanics Symposium*, Tonon, F. & Kottenstette, J.T. (Eds), Colorado School of Mines. p. 33-48.
- Geertsema, A.J. (2002): The shear strength of planar joints in mudstone. *Int. J. Rock Mech. Min. Sci.* 39: 1045-1049.
- Gehle, C. (2002): Bruch- und Scherverhalten von Gesteinstrennflächen mit dazwischenliegenden Materialbrücken, *Schriftenreihe des Lehrstuhls für Grundbau, Boden- und Felsmechanik*, 33. Ruhr-Universität Bochum.
- Geology Café (2013): Introduction to Geology: Chapter 6 - Fault Systems and Earthquakes. <http://www.geologycafe.com/images/strike-n-dip.jpg> last accessed 06.12.2018

- Geology Field Camp (2013): South Dakota School of Mines & Technology, <http://geologyfieldcamp.sdsmt.edu/Photogallery%202007.Htm> last accessed: 06.12.2018
- Gomez, J.E.; Filz, M.G.; Ebeling, R.M. & Dove, J.E. (2008): Sand-to-Concrete interface response to Complex load paths in a large displacement shear box. *Geotechnical Testing Journal*, 31(4): 1-12.
- Grasselli, G. & Descoeurdes, F. (2001): Shear strength of rock joints based on quantified surface description, In: *Infoscience EPFL scientific publications*, Ecole Polytechnique Federale de Lausanne. 126 p.
- Haneberg, W.C. (2008): Using close range terrestrial digital photogrammetric for 3D rock slope modeling and discontinuity mapping in the United States. *Bulletin of Engineering Geology and the Environment.*, 67(4): p. 457-469.
- Hong, E.S.; Lee, I.M. & Lee, J.S. (2006): Measurement of rock joint roughness by 3D scanner. *Geotechnical testing Journal*, 29(6).
- Hong, E.S.; Lee, J.S. & Lee, I.M. (2008): Underestimation of roughness in rough rock joints. *Int. J. Numer. Anal. Meth. Geomech.* 32(11): 1385-1403.
- ISRM (1978): International society for rock mechanics commission on standardization of laboratory and field tests: Suggested methods for the quantitative description of discontinuities in rock masses. *Int J Rock Mech Min Sci Geomech Abstr*, 15(6): 319-368.
- Jaeger, J.C. & Rosengren, K.J. (1969): Friction and sliding of joints. *Proc. Aust. Inst. Min. Metall.* 229, 93-104.
- Jessell, M.W.; Cox, S.J.D.; Schwarze, P. & Power, W.L. (1995): The anisotropy of surface roughness measured using a digital photogrammetric technique. *Geological Society London. Special Publications*, 92(1): 27-37.
- Jiang, Y.; Xiao, J.; Tanabashi, Y. & Mizokami, T. (2004): Development of an automated servo-controlled direct shear apparatus applying a constant normal stiffness condition. *Int. J. Rock Mech. Min. Sci.*, 41: 275-286.
- Kim, D.Y.; Chun, B.S. & Yang, J.S. (2006) Development of a direct shear apparatus with rock joints and its verification tests. *Geotechnical Testing*, 29(5).
- Konietzky, H.; Frühwirth, T. & Nguyen, V.M. (2012a): GS 1000: A new large rock-mechanical shear box device for dynamic and HM-coupled testing under extreme strong forces. *Rock Engineering and Technology for Sustainable Underground Construction EUROCK 2012*, International Society for Rock Mechanics and Rock Engineering.
- Konietzky, H.; Frühwirth, T. & Luge, H. (2012b): A new large dynamic rockmechanical direct shear box device. *Rock Mechanics Rock Engineering*, 45(3): 427-432
- Kulatilake, P.H.S.W.; Shou G.; Huang, T.H. & Morgan, R.M. (1995) New peak shear strength criteria for anisotropic rock joints. *Int. J. Rock Mech. Min. Sci.*, 32(7): 673-697.
- Lee, H.S. & Ahn, K.W. (2004): A prototype of digital photogrammetric algorithm for estimating roughness of rock surface. *Geosciences Journal*, 8(3): 333-341.
- Maerz, N.H.; Franklin, J.A. & Bennett, C.P. (1990): Joint roughness measurement using shadow profilometry. *Int. J. Rock Mech. Min. Sci.*, 27(5): 329-343.
- Milne, D.; Germain, P.; Grant, D. & Noble, P. (1991): Field observation for the standardization of the NGI classification system for underground mine design In: *International Congress on Rock Mechanics*, A.A. Balkema, Aachen, Germany.

- Nasseri, M.H.B.; Tatone, B.S.A.; Grasselli, G. & Young, R.P. (2009): Fracture toughness and fracture roughness interrelationship in thermally treated Westerly granite. *Pure and Applied Geophysics*, 166(5-7): 801-822.
- Nguyen, V.M. (2013): Static and dynamic behaviour of joints in schistose rock: lab testing and numerical simulation, *Publ. Geotechnical Institute 2013-3*, ed. H. Konietzky, TU Bergakademie Freiberg, Germany.
- Nilsson, M.; Edelbro, C. & Sharrock, G. (2012): Small scale joint surface roughness evaluation using digital photogrammetry. *Rock Engineering and Technology for Sustainable Underground Construction EUROCK 2012*, International Society for Rock Mechanics and Rock Engineering.
- Patton, F.D. (1966): Multiple modes of shear failure in rock. *Proc. 1st congress Int. Soc. Rock Mech.*, Lisbon 1, 509-513.
- Poropat, G.V. (2009): Measurement of surface roughness of rock discontinuities, in Rock engineering in difficult conditions. *Proc. of 3rd Canada-US Rock mechanics Symposium 2009*.
- Rasouli, V. & Harrison, J.P. (2004): A comparison of linear profiling and an in-plane method for the analysis of rock surface geometry. *Int. J. Rock Mech. Min. Sci.*, 41(3): 377-378.
- Shigui, D.; Yunjin, H. & Xiaofei, H. (2009): Measurement of joint roughness coefficient by using profilograph and roughness ruler. *Journal of Earth Science*, 20(5): 890-896.
- Schmittbuhl, J.; Gentier, S. & Roux, S. (1993) Field measurements of the roughness of fault surfaces. *Geophysical Research Letters*, 1993. 20(8): 639-641
- Seidel, J.P. & Haberfield, C.M. (2002): Laboratory testing of concrete-rock joints in Constant Normal Stiffness direct shear. *Geotechnical testing*, 25(4): 391-404.
- Tatone, S.A. & Grasselli, G. (2009): Use of a stereo-topometric measurement system for the characterization of rock joint roughness in-situ and in the laboratory, in Rock engineering in difficult conditions. *Proc. of 3rd Canada-US Rock mechanics Symposium 2009*.
- Tatone, S.A. & Grasselli, G. (2013): An investigation of discontinuity roughness scale dependency using high-resolution surface measurements. *Rock mechanics and Rock engineering*, 46(4): 1-25.
- Tonon, F. & Kottenstette, J.T. (2006): Laser and photogrammetric methods for rock face characterization: a workshop. In: *Laser and Photogrammetric methods for Rock face characterization*. American Rock Mechanics Association, Alexandria. pp 5-10.
- Tse, R. & Cruden, D.M. (1979): Estimating joint roughness coefficients. *Int. J. Rock Mech. Min. Sci.*, 16(5): 303-307.
- Weissbach, G. (1978): A new method for the determination of the roughness of rock joints in the laboratory. *Int. J. Rock Mech. Min. Sci.*, 15(3):131-133.
- Wickens, E.H. & Barton, N.R. (1971): The application of photogrammetry to the stability of excavated rock slopes. *The Photogrammetric Record*, 7(37): 46-54
- Yang, Z.; Lo, S.C. & Di, C.C. (2001): Reassessing the joint roughness coefficient (JRC) estimation using Z2. *Rock mechanics and Rock engineering*, 34(3): 243-251.